MAGNETO-OPTICAL PROPERTIES OF ARRAYED STRUCTURES OF CYLINDRICAL AND ELLIPTICAL QUANTUM DOTS

[1]Lilit YEGANYAN, [2]Maryam MANSOURY, [1]Vram MUGHNETSYAN

[1]Center for Modeling and Simulations of Nanostructures, Research Laboratory of Solid State Physics, Institute of Physics, Yerevan State University, Yerevan, Armenia, lilit.yeganyan@ysu.com, vram@ysu.am

[2]Department of Physics, Urmia University of Technology, Urmia, Iran, mansourymaryam.uut@gmail.com

https://doi.org/10.37904/nanocon.2023.4768

Abstract

In this paper we present a comparative study of the magneto-optical properties of quasi-two-dimensional electrons in a graphene-like semiconductor superlattice composed of circular and elliptical quantum dots. The effect of transverse magnetic field on the band structure and absorption coefficient of the considered structures is studied. To this end a complete set of orthogonal basis functions is constructed in the symmetric gauge of the vector potential. This basis reflects both the periodicity of the system and magnetic phase effects due to the translations between the sites of the superlattice. Our calculations indicate on a topological change in the miniband structure due to the ellipticity of the quantum dots, and non-trivial modifications of the electron energy dispersion surfaces in the reciprocal space with the change of the number of magnetic flux quanta through the unit cell of the superlattice. The obtained results indicate the opportunity for an effective control of the magnetic and optical characteristics of honeycomb arrays of QDs through geometry effects and external magnetic field.

Keywords: Artificial graphene, Magnetic field, Energy dispersion, Absorption coefficient

INTRODUCTION

The unique properties of graphene, which are a direct consequence of its two-dimensional (2D) lattice with underlying triangular symmetry, have attracted significant interest in recent two decades [1]. Advanced methods, such as atom-by-atom assembly [2], optical trapping of ultracold atoms in crystals of standing light waves [3], and nanopatterning of 2D electron gas in semiconductors [4], make it possible to design and fabricate artificial honeycomb lattices or artificial graphene. In artificial graphene composed of semiconductor quantum dots (QD) there are additional possibilities of band structure manipulation via variations of the QD shapes, sizes and external factors such as transverse magnetic and in-plane electric fields [5]. The description of the electron motion in graphene subjected to a transverse homogeneous magnetic field is usually based on the Peierls substitution in tight-binding models or the Dirac Hamiltonian [6]. This approach relies on the assumption that the magnetic field affects the tunneling of an electron through the sites of the graphene lattice only by adding corresponding magnetic phases to the hopping parameters. The Dirac Hamiltonian is applicable when there is only one conducting electron in each site of the lattice, leading to the emergence of relativistic electrons near the band's touching points. These assumptions, while well justified for graphene, may not hold for artificial graphene-like semiconductor structures. To overcome this obstacle, we develop our theoretical study using the basis functions proposed initially by Ferrari [7] and subsequently used by others. This approach allows us to take into account the effect of the magnetic field on the degree of confinement of electrons in each QD, as well as on the tunneling of 2D electrons between different QDs [8]. Based on this method, we investigate the electronic states and the absorption coefficient of honeycomb artificial graphene-like lattices composed of cylindrical and elliptical QDs. We explore the effect of structural symmetry-breaking on energy dispersions and the optical response of the lattice. Our calculations indicate a topological change in the miniband structure due to the ellipticity of the QD and non-trivial modifications of the electron energy dispersion surfaces in reciprocal space with the change of the number of magnetic flux quanta through the unit cell (UC) of the superlattice (SL). It is shown that the magnetic field dramatically alters the band structure and, consequently, the optical absorption spectrum of the lattice. The obtained results indicate the opportunity for effective manipulation of the optical characteristics of honeycomb arrays of QDs through their geometry and external magnetic field.

1. THEORETICAL FRAMEWORK

We consider a 2D lattice composed of planar QDs exposed to a transverse homogeneous magnetic field with induction B. The one-electron Hamiltonian of such a system in the effective mass approximation is

$$H = H_0 + V(r) \tag{1}$$

where

$$H_0 = \frac{1}{2m}\left(\boldsymbol{p} + \frac{e\boldsymbol{A}}{c}\right)^2 \tag{2}$$

and $V(r) = V(\boldsymbol{r} + n_1\boldsymbol{a}_1 + n_2\boldsymbol{a}_2)$ is the periodic potential of the SL with primitive vectors $\boldsymbol{a_1}$ and $\boldsymbol{a_2}$, and with integer n_1 and n_2. $\boldsymbol{p} = -i\hbar\boldsymbol{\nabla}$ is the momentum operator, $\hbar$ is the reduced Planck's constant, m is the effective mass, and c is the speed of light. We assume that the SL consists of circular or elliptical QDs (see Figure 1) with a rectangular potential profile. Namely, $v(\boldsymbol{r}) = v_0$ ($v_0 < 0$) inside each QD and $v(\boldsymbol{r}) = 0$ in the surrounding medium. For the symmetric gauge of the vector potential: $A = (B/2)(-y, x)$the eigenfunctions of the Hamiltonian (2) are

$$\varphi_{n,L}(r) = \frac{1}{\sqrt{2\pi l_B^2 n_{L!}}}\left(\frac{x+iy}{\sqrt{2}l_B}\right)^{nL} e^{\frac{-r^2}{4l_B^2}}, \tag{3}$$

where $l_B = (c\,\hbar/eB)^{1/2}$ is the magnetic length, and n_L indicates the number of the Landau level [7,9]. It is well known that the translation operator $T(\boldsymbol{R}) = \exp\,(i\boldsymbol{Rp}/\hbar)$ with $\boldsymbol{R} = n_1\boldsymbol{a_1} + n_2\boldsymbol{a_2}$ does not commute with the Hamiltonian (2). Instead, the so-called magnetotranslation operator $S(\boldsymbol{R}) = exp\big((i/2l_B^2)(\boldsymbol{R}\times\boldsymbol{r})\hat{e}_z\big)T(\boldsymbol{R})$ [7,10] which commutes with the Hamiltonian (2) can be used for construction of a complete and orthogonal set of basis functions for description of the motion of an electron with the Hamiltonian (1). On the other hand, magnetotranslation operators for any two lattice vectors $\boldsymbol{R_1}$ and $\boldsymbol{R_2}$ commute in the only case when there is an integer number of magnetic flux quanta in the area $|\boldsymbol{R_1}\times\boldsymbol{R_2}|$: $[S(\boldsymbol{R_1}), S(\boldsymbol{R_2})] = 0, if\,|\boldsymbol{R_1}\times\boldsymbol{R_2}| = 2\pi u l_B^2$, where u is an integer. If one expresses the magnetic flux per UC of the SL as $\Phi/\Phi_0 = pq/h_1h_2$, where p, q, h_1 and h_2 are integers, the lattice vectors satisfying this condition should be expressed as follows: $\boldsymbol{R_1} = h_1\boldsymbol{a_1}$ and $\boldsymbol{R_2} = h_2\boldsymbol{a_2}$. As is shown in [8] a complete set of basis functions can be constructed out using the primitive magnetotranslations $S(\boldsymbol{c})$ and $S(\boldsymbol{d})$ with $\boldsymbol{c} = \boldsymbol{R_1}/p$ and $\boldsymbol{d} = \boldsymbol{R_2}/p$:

$$\phi_{n_L}^{n_1,n_2}(r) = (pq)^{-1/2}\sum_{m,n=-\infty}^{\infty}[S(\boldsymbol{c})e^{-i\mu}]^m\,[S(\boldsymbol{d})e^{-iv}]^n\phi_{nL}(\boldsymbol{r}), \tag{4}$$

where

$$\mu = (1/p)(\theta_1 + 2\pi n_1), n_1 = 0, \dots, p-1, \tag{5}$$

$$v = (1/q)(\theta_2 + 2\pi n_2), n_2 = 0, \dots, p-1,$$

θ_1 and θ_2 indicate points in the magnetic first Brillouine zone (FBZ). It has been shown that the norm of the wave function (6), is nonzero when $(\mu, v) \neq (\pi, \pi)$ [8,11]. The periodic potential of SL can be expanded in a Fourier series with reciprocal lattice vectors $\boldsymbol{G} = G_1\boldsymbol{g_1} + G_2\boldsymbol{g_2}$, where $\boldsymbol{g_1}$ and $\boldsymbol{g_2}$, are the primitive reciprocal vectors and G_1 and G_2 are integers. The Fourier transform of the honeycomb lattice potential with distance a between QDs and with the area of UC s_0 can be expressed as follows:

$$v(\boldsymbol{G})_{cyl} = \begin{cases} \dfrac{v_0}{s_0} 2\pi r_d^2 \ if \ G_1 = G_2 = 0; \\ \dfrac{v_0}{s_0} e^{-i\frac{2\pi}{3}(G_1+G_2)} \left(1 + e^{-i\frac{2\pi}{3}(G_1+G_2)}\right) \times \dfrac{3 r_d a}{\sqrt{(G_1+G_2)^2 + 3(G_1-G_2)^2}} \\ \qquad \times J_1\left(\dfrac{2\pi r_d \sqrt{(G_1+G_2)^2 + 3(G_1-G_2)^2}}{3a}\right), \text{otherwise} \end{cases} \tag{6}$$

for the SL of circular QDs with radius r_d, and

$$v(\boldsymbol{G})_{el} = \frac{v_0}{s_0} e^{-i\frac{2\pi}{3}(G_1+G_2)} \left(1 + e^{-i\frac{2\pi}{3}(G_1+G_2)}\right) \times \int_0^{r_e} \int_0^{2\pi} e^{-i\frac{2\pi}{3a} r\left((\cos\phi + \sqrt{3}\sin\phi)G_1 + (\cos\phi - \sqrt{3}\sin\phi)G_2\right)} r dr d\phi \,, \tag{7}$$

for the SL of elliptical QDs, where $r_e = r_s r_l / \sqrt{r_s^2 \cos^2\phi + r_l^2 \sin^2\phi}$, $r_{s(l)}$ is the small (large) semi-axis of the QD. The matrix elements of the exponent in the Fourier expansion of the potential are non-zero if:

$$G_1 h_1 + n_1 - n_1' = Mp \tag{8}$$

$$G_2 h_2 + n_2 - n_2' = Nq,$$

with M and N integers [7,10].

The absorption coefficient in the dipole approximation can be expressed as follows:

$$\alpha(\omega) = \alpha_0 \sum_{i,f} \left|\langle \psi_f | \vec{\varepsilon}\vec{p} | \psi_i \rangle\right|^2 \delta(\varepsilon_f - \varepsilon_i - \hbar\omega)\left[f(\varepsilon_i) - f(\varepsilon_f)\right], \tag{9}$$

where $\alpha_0 = 4\pi e^2 \hbar / nc\, {m_0}^2 L_z$, m_0 stands for the free electron mass, $\langle \psi_f | \vec{\varepsilon}\vec{p} | \psi_i \rangle$ is the transition matrix element, $f(\varepsilon_j)$ is the Fermi-Dirac distribution function and L_z is the effective width of the absorbing medium.

2. RESULTS AND DISCUSSION

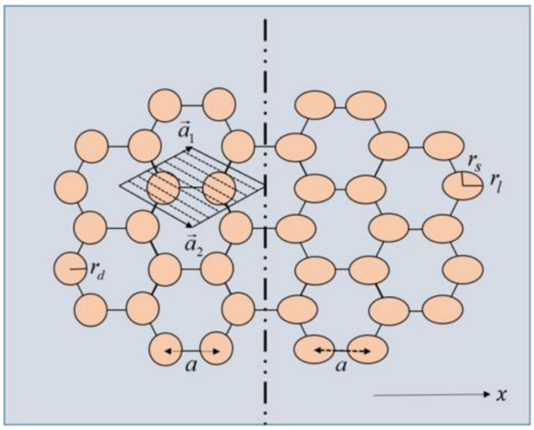

Figure 1 The schematic view of the 2D SLs of circular (the left half of the figure) and elliptical (the right half of the figure) QDs.

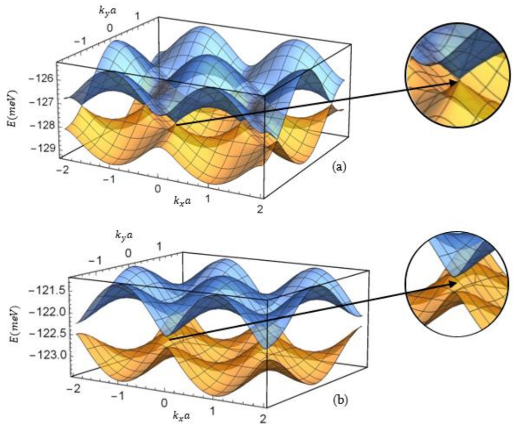

Figure 2 Electron energy dispersion surfaces in the absence of external magnetic field for SLs composed of circular (upper figure) and elliptical (lower figure) QDs**.**

Figure 2 shows the dispersion surfaces for circular (a) and elliptical (b) QDs for the first two minibands in the absence of magnetic field. In the case of circular QDs (**Figure 2a**), the minibands have touching points with degenerate energy. The energy dispersion around these points is linear, which indicates on the relativistic behavior of electron. The symmetry of the dispersion surfaces in this case is hexagonal. In the case of elliptical

QDs, the hexagonal symmetry is broken. As a result a finite band gap appears between the minibands, which significantly affects the optical characteristics of the system.

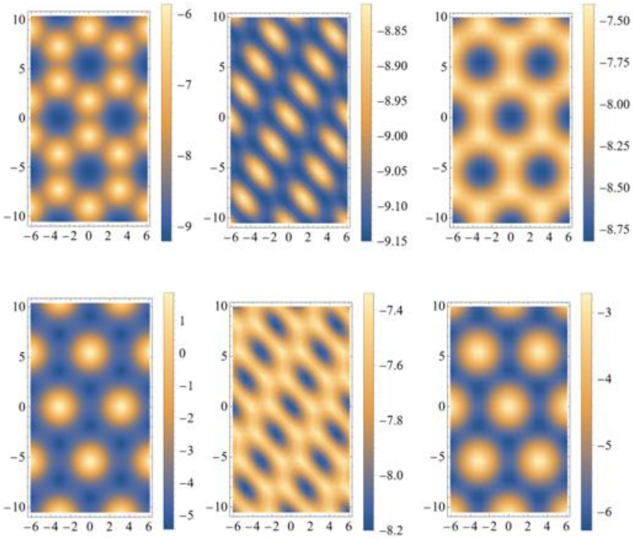

Figure 3 Dispersion surfaces for the first (upper row) and the second (lower row) miniband in honeycomb SL of circular QDs. The horizontal axis in each panel is for and the vertical axis is for. The magnetic flux in the unites of flux quantum is and for the left, middle and the right columns, respectively. The energy is expressed in.

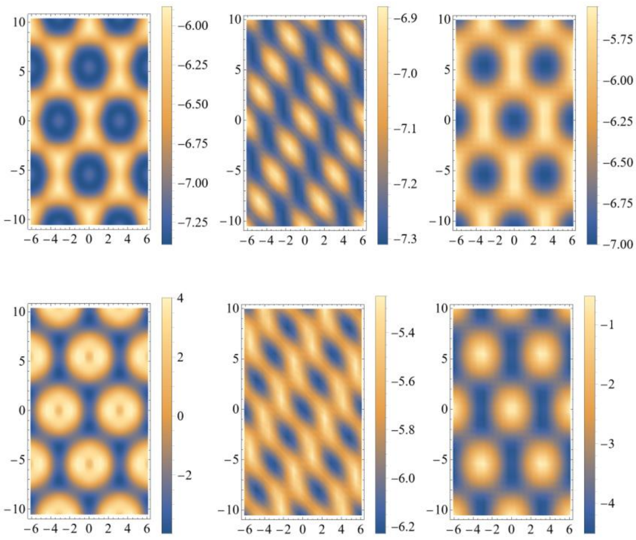

Figure 4 Dispersion surfaces for the first (upper row) and the second (lower row) minibands in honeycomb SL of elliptical QDs. The horizontal axis in each panel is for and the vertical axis is for. The magnetic flux in the unites of flux quantum is and for the left, middle and the right columns, respectively.

Figure 3 represents the density plots of the dispersion surfaces for a SL composed of circular QDs. The considered values of the magnetic flux per UC are $\phi/\phi_0 = 1, 3/2$ and 2, respectively for the left, the middle and the right columns in the figure. The upper row of the figure corresponds to the 1st, while the lower row is for the 2nd miniband. First of all it is obvious that the dispersion surfaces retain their triangular symmetry when there is integer number of magnetic flux quanta per UC (the left and the right columns of the **Figure 3**). However, the fractional number of flux quanta per UC leads to the destruction of the triangular symmetry. For $\phi/\phi_0 = 3/2$ one of the lattice vectors of the system with magnetic field is the twice of the original lattice vector, which leads to the contraction of the period in the reciprocal space two times (see the middle column of **Figure 3**). Another interesting phenomenon is the shift of the positions in the FBZ of maxima and minima of the dispersion surfaces corresponding to even and odd numbers of flux quanta per UC with regard to each other In all the cases with non-zero magnetic field a finite gap between the minibands is opened, whic is a result of the magnetic-phase interference between the states localized in two QDs in the same UC.

In **Figure 4** the same as in **Figure 3**, but for a SL composed of elliptical QDs is presented. In this case the SL has a rectangular symmetry, which is not destroyed by the magnetic field when there is an integer number of flux per UC. The energy values shown on the legends of the figure indicate on the decrease of the gap between the minibands with the increase of the magnetic flux. One can also observe that the rectangular symmetry is better expressed for larger integer numbers of magnetic flux per UC (compare the left and the right columns of the **Figure 4**).

The absorption spectra of the honeycomb lattice composed of circular (solid lines) and elliptical (dotted lines) QDs are presented in **Figure 5** for the 1 (a), 2 (b) and 3/2 (c) flux quanta per UC. We consider four different directions of the photon polarization with regard to x axis as is mentioned in the figure. It is obvios that the photon polarization has a significant effect on the absorption intensity and smaller intensities are observed when the polarization has the direction of stronger tunneling between nearest QDs. For $\phi/\phi_0 = 1$ and $\phi/\phi_0 = 2$ (**Figures 5a and 5b**) the deviation of the QD geometry from circular one leads to the appearence of additional maxima in the absorption specrtum. For $\phi/\phi_0 = 3/2$ the behavior of the curves which correspond to different QD geometry are similar but the values of absorption coefficient are strongly different, in contrast to the cases shown in **Figures 5a and 5b**. The comparison of all three Figures shows that the change of the magnetic flux per UC of the SL dramatically alters both the absorption intensity and the incident photon energy range where the absorption is significant. Note that the absorption intensity varies non-monotonically with the increase of the number of magnetic flux quanta per UC.

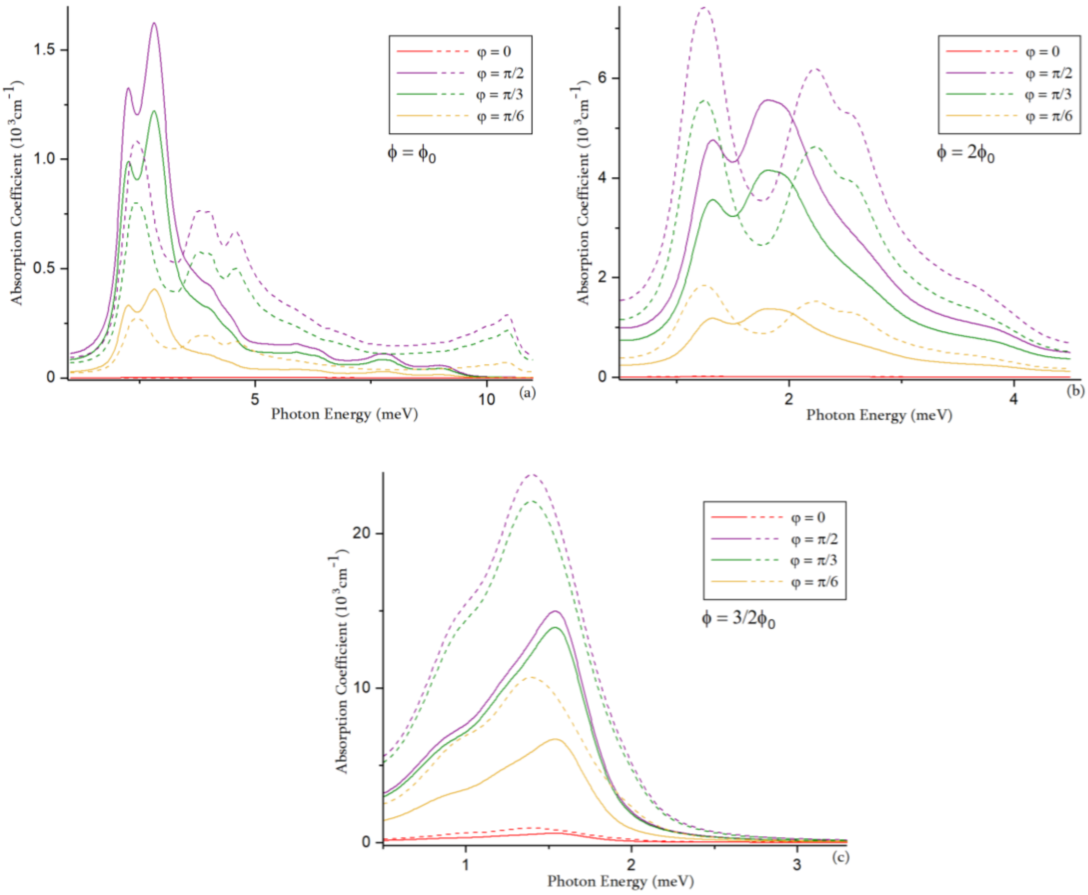

Figure 5 Dependencies of the absorption coefficient on incident photon energy for different polarizations of the incident photon and different values of magnetic flux through the UC of SL for elliptical and circular QDs. The solid lines correspond to the case of circular QDs, while the dashed ones are plotted for elliptical QDs.

3. CONCLUSION

Summarizing, we present a comparative study on electron energy dispersions and the magnetoabsorption of artificial graphene-like honeycomb SLs composed of circular and elliptical QDs. We develop our theoretical model in the frame of the approach proposed earlier by Ferrari, where a complete orthonormal set of basis wave functions is used, which reflects both the SL translational symmetry and the wave function phase-shifts due to the transverse magnetic field in the symmetric gauge of the vector potential. Our calculations indicate a topological change in the miniband structure due to the ellipticity of QDs. We observe non-trivial displacements in the reciprocal space of the energy dispersion surfaces and transformations in the translational symmetry of the system when passing through different rational values of the number of magnetic flux quanta per UC of the SL. The absorption coefficient significantly depends on the number of magnetic flux quanta per UC of the SL and on the polarization of incident photon. The deviation of the QDs geometry form a circular one leads to qualitative changes in the absorption spectrum for integer numbers of magnetic flux quanta per UC. Meanwhyle, for half an integer values of magnetic flux quanta there are almost no qualitative but instead there are strong quantitive modifications in the absorprion spectrum. The obtained results indicate the opportunity for effective and flexible manipulation of the magnetic and optical characteristics of honeycomb arrays of QDs through geometry effects and external magnetic field.

ACKNOWLEDGEMENTS

This work was financially supported by the Armenian State Committee of Science (grants No 21SCG-1C012 and No 21T-1C247).

REFERENCES

[1] GEIM, A.K., NOVOSELOV, K.S. The rise of graphene in nanoscience and technology: a collection of reviews from nature journals. *World Sci.* 2010, vol. 11–9.

[2] GOMEZ, K.; MAR, W.; KO, W.; GUINEA, F.; MANOHARAN, H.C. Designer Dirac fermions and topological phases in molecular graphene. *Nature.* 2012, vol. 483, no. 306.

[3] TARRUELL, L., GREIF, D., UEHLINGER, T., JOTZU, G., ESSLINGER, T. Creating, moving and merging Dirac points with a Fermi gas in a tunable honeycomb lattice. *Nature.* 2012, vol. 483, no. 302.

[4] SINGHA, A.; GIBERTINI, M.; KARMAKAR, B.; YUAN, S.; POLINI, M.; VIGNALE, G.; KATSNELSON, M. I.; PINCZUK, A.; PFEIFFER, L.N.; WEST, K.W.; PELLEGRINI, V. Two-Dimensional Mott-Hubbard Electrons in an Artificial Honeycomb Lattice. *Science.* 2011, vol. 332, no. 1176.

[5] MUGHNETSYAN, V.; MANASELYAN, A.; BARSEGHYAN, M.; KIRAKOSYAN, A.; LAROZE, D. Rashba splitting of Dirac points and symmetry breaking in strained artificial graphene. *Physical Review B.* 2019, vol. 100, 195132.

[6] GOERBIG, M.O. Electronic properties of graphene in a strong magnetic field. *Reviews of Modern Physics.* 2011, vol. 83, 1193.

[7] FERRARI R. Two-dimensional electrons in a strong magnetic field: A basis for single-particle states. *Physical Review B.* 1990, vol. 42, 4998.

[8] MANSOURY, M.; MUGHNETSYAN, V.; MANASELYAN, A.; KIRAKOSYAN, A.; GUDMUNDSSON, V.; AZIZ-AGHCHEGALA, V. Hofstadter-like spectrum and magnetization of artificial graphene constructed with cylindrical and elliptical quantum dots. *Physics Letters* A. 2023, vol. 487, 129115.

[9] LANDAU, L.D., LIFSHITZ, E.M. *Quantum mechanics: nonrelativistic theory (3rd ed.).* Amsterdam: Butterworth Heinemann. pp. 424–426.

[10] SILBERBAUER H., Magnetic minibands in lateral semiconductor superlattices. *Journal of Physics: Condensed Matter* 1992, vol .7355, no. 4.